Phenomenology of modified loop quantum cosmology

Bao-Fei Li

Institute for Theoretical Physics & Cosmology
Zhejiang University of Technology
This lecture is based on the work with Meysam Motaharfar, Javier Olmedo, Parampreet Singh and Anzhong Wang.

May 20, 2026

Outline

1.1 Inflation

➢ Inflation [1] is an extremely rapid (exponentially) expansion of the universe after its creation ($t \simeq 10^{-34}\ s$):

$$a(t) = a_i e^{H(t-t_i)} \qquad \text{(A. Guth, 1981)}$$

where a is the scale factor of the universe and $H = \dot{a}/a$ is the Hubble parameter.

- For the spatially-flat homogeneous and isotropic Friedmann-Lemaître-Robertson-Walker (FLRW) universe, the metric is simply given by

$$ds^2 = -dt^2 + a^2 d\vec{r}^2.$$

[1] For review, See D. Baumann, Cosmology, 2022.

1.1 Inflation

- As the universe experiences exponential expansion during inflation, we usually use the number of e-foldings which is defined below to describe how much the universe has expanded during the inflationary phase,

$$N_{\rm inf} = \ln\left(\frac{a_{\rm end}}{a_i}\right).$$

- For a universe filled with a perfect fluid with the equation of state $\omega = P/\rho$, the co-moving Hubble horizon behaves as

$$(aH)^{-1} \propto a^{\frac{1}{2}(1+3\omega)}.$$

1.1 Inflation

- The co-moving Hubble horizon monotonically increases for non-relativistic matter ($\omega = 0$) and radiation ($\omega = 1/3$), while it monotonically decreases during inflation ($\omega \approx -1$).

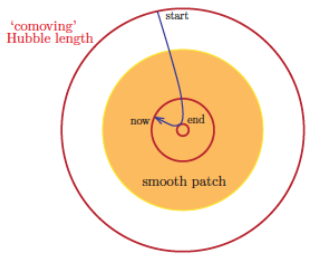

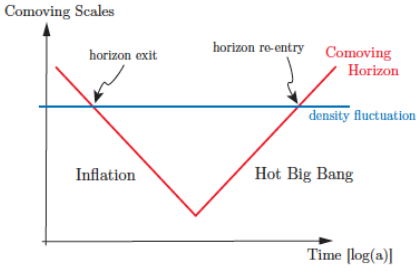

1.1 Challenging (Theoretical) Problems

However, inflation is also facing various challenging (theoretical) problems:

- Initial singularity problem: General relativity (GR) inevitably leads inflation to an initial singularity [2].
  - For example,

$$a(t) = a_i t^{\alpha}, \quad \alpha > 0$$
$$\Rightarrow H^2 = \left(\frac{\dot{a}}{a}\right)^2 = \frac{\alpha^2}{t^2}$$
$$\Rightarrow \rho = \left(\frac{3}{8\pi G}\right)\frac{\alpha^2}{t^2} \to \infty, \quad \text{as} \quad t \to 0$$

[2] A. Borde and A. Vilenkin, PRL72 (1994) 3305; A. Borde, A. H. Guth, and A. Vilenkin, PRL90 (2003) 151301.

1.1 Challenging (Theoretical) Problems

➢ Trans-Planckian Problem [3]:

- To be consistent with observations, we need

$$N_{\text{inf}} \geq 60.$$

- From the end of inflation to the present, $N_0 \approx 60$. Thus,

$$\lambda_{\text{Ob.}} < \ell_{Pl} \equiv 10^{-35} m,$$

that is, the wavelengths corresponding to present observations, should be smaller than the Planck length at the beginning of the inflation, and quantum gravity becomes important.

✯ Quantum aspects of gravity should be taken into account in order to solve the big-bang singularity and the initial condition problems in the standard cosmology model.

[3] Brandenberger and Martin, CGQ30 (2013) 113001.

1.2 Loop quantum cosmology

- Loop quantum cosmology [4] (LQC) provides a mathematically rigorous framework to generically resolve the classical singularities in various cosmological spacetimes, including the FLRW universe, the Bianchi universe, the Gowdy models and etc.
- Symmetry reduction of the connection and triad variables in cosmological spacetimes leads to managenable quantum Hamiltonian constraints and the quantum difference equations which govern the evolution of the spacetimes[5].
- For the purpose of the phenomenological investigation of the cosmological implications of LQC, the effective dynamics is always employed.

[4] For review see A. Ashtekar and P. Singh, Class. Quant. Grav. 28, 213001 (2011),arXiv:1108.0893, I. Agullo and P. Singh, arXiv:1612.01236 and references therein.

[5] Ashtekar,Pawlowski and Singh, PRL 96, 141301 (2006); PRD 73,124036(2006);PRD 74,084003 (2006).

1.2 Loop quantum cosmology

➢ The gravitational Hamiltonian constraint consists of the so-called Euclidean and Lorentzian terms [6],

$$\begin{aligned}
\mathcal{H}_{\rm grav} &= \mathcal{H}^{(E)}_{\rm grav} - (1+\gamma^2)\mathcal{H}^{(L)}_{\rm grav}, \\
\mathcal{H}^{(E)}_{\rm grav} &= \frac{1}{16\pi G}\int {\rm d}^3x\, \epsilon_{ijk} F^i_{ab} \frac{E^{aj}E^{bk}}{\sqrt{|{\rm det}(q)|}}, \\
\mathcal{H}^{(L)}_{\rm grav} &= \frac{1}{8\pi G}\int {\rm d}^3x\, K^j_{[a}K^k_{b]} \frac{E^{aj}E^{bk}}{\sqrt{|{\rm det}(q)|}},
\end{aligned}$$

where γ is the Barbero-Immirzi parameter, q_{ab} is the spatial metric, A^i_a is the Ashtekar-Barbero connection, F_{ab} is the field strength and K^i_a is the extrinsic curvature.

[6] Jakub Mielczarek, Tomasz Stachowiak, Marek Szydlowski, Phys. Rev. D77 (2008) 123506; Pietro Dona, Simone Speziale, arXiv: 1007.0402.

1.2 Loop quantum cosmology

- In the homogeneous and isotropic spatially-flat FLRW universe, we have

$$A_a^i \sim c = \gamma \dot{a}, \ E_i^a \sim p = a^2.$$

Therefore in terms of c and p,

$$\mathcal{H}_{\rm grav}^{(E)} = \frac{3p^{1/2}c^2}{\kappa}, \ \ \mathcal{H}_{\rm grav}^{(L)} = -\frac{3p^{1/2}c^2}{\kappa}\left(1+\frac{1}{\gamma^2}\right),$$

where $\kappa = 8\pi G$.

- In standard LQC, only the Euclidean term $\mathcal{H}_{\rm grav}^{(E)}$ is quantized, leading to the quantum Hamiltonian constraint and the quantum difference equation which governs the evolution of a quantum cosmos[7].

[7] A. Ashtekar, T. Pawlowski and P. Singh, Phys. Rev. **D**74 (2006) 084003.

1.2 Loop quantum cosmology

- For the phenomenological investigations of the cosmological implications of LQC, we appeal to the effective dynamics based on the effective Hamiltonian constraint.
  - The classical Hamiltonian constraint assumes

$$\mathcal{H}_{classical} = -\frac{3p^{1/2}c^2}{\kappa\gamma^2}.$$

  - In the $\bar{\mu}$ scheme, the connection is polymerized as $c \to \frac{\sin(\bar{\mu}c)}{\bar{\mu}}$ with $\bar{\mu} = \frac{\lambda}{\sqrt{p}}$.
- The resulting effective Hamiltonian is given by,

$$\mathcal{H}_{LQC} = -\frac{3v\sin^2(\lambda b)}{8\pi G\gamma^2\lambda^2}, \quad \left(v = a^3;\ b = \frac{c}{\sqrt{p}}\right) \to \mathcal{H}_{classical} = -\frac{3vb^2}{8\pi G\gamma^2}.$$

where $\lambda^2 \equiv 4\sqrt{3}\pi\gamma\ell_{PL}^2$ and $\{b, v\} = 4\pi G\gamma$.

1.2 Loop quantum cosmology

- For the matter sector, we assume a single scalar field for the most pragmatic purpose

$$\mathcal{H}_M = \frac{p_\phi^2}{2v} + vV(\phi),$$

where p_ϕ is the conjugate momentum of the inflaton field.

- Then, we obtain the following Hamilton's equations

$$\begin{aligned}
\dot{v} &= \left\{v, \mathcal{H}_{LQC} + \mathcal{H}_M\right\} = \frac{3v}{2\lambda\gamma}\sin(2\lambda b), \\
\dot{b} &= \left\{b, \mathcal{H}_{LQC} + \mathcal{H}_M\right\} = -4\pi G\gamma(\rho + P), \\
P &\equiv -\frac{\partial \mathcal{H}_{\mathcal{M}}}{\partial v}, \quad \rho \equiv \frac{\mathcal{H}_{\mathcal{M}}}{v} = \rho_c \sin^2(\lambda b), \\
\rho_c &\equiv \frac{\sqrt{3}\rho_{\rm Pl}}{32G\pi^2\gamma^3\ell_{\rm Pl}^2} \approx 0.41\rho_{\rm Pl}.
\end{aligned}$$

1.2 Loop quantum cosmology

- From the Hamilton's equations,

$$H^2 = \frac{\dot{v}^2}{9v^2} = \frac{\sin^2(2\lambda b)}{4\lambda^2\gamma^2} = \frac{8\pi G}{3}\rho\left(1 - \frac{\rho}{\rho_c}\right).$$

- The big bang singularity is replaced by a quantum bounce at $\rho = \rho_c$ [8] where $H = 0$ and $\ddot{a} > 0$.
- The momentum b is a monotonically decreasing function during the forward evolution of the universe in time. At the bounce, $b = \frac{\pi}{2\lambda}$.

[8] A. Ashtekar, P. Singh, CQG28 (2011) 213001.

1.2 Loop quantum cosmology

- In this figure we compare the evolution of the universe in the classical cosmology with that in LQC when a massless scalar field is considered in the matter sector.

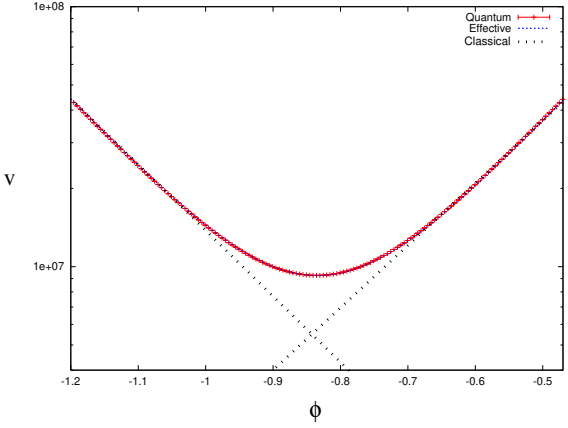

[Li and Singh, arXiv:2304.05426]

2. The background dynamics of the modified loop quantum cosmology

2.1 The effective dynamics of mLQC

☞ As early as in 2009, separate treatments of the Lorentzian term in the reference [J. Yang,Y.Ding and Y. Ma, PLB682 (2009) 1] yielded two alternative LQC models.

- mLQC-I:

$$b_{\rm I}^2 \to -\frac{\gamma^2}{\lambda^2}\Big\{\sin^2(\lambda b) - \frac{\gamma^2+1}{4\gamma^2}\sin^2(2\lambda b)\Big\},$$

- mLQC-II:

$$b_{\rm II}^2 \to \frac{4}{\lambda^2}\sin^2\left(\frac{\lambda b}{2}\right)\left\{1+\gamma^2\sin^2\left(\frac{\lambda b}{2}\right)\right\}.$$

☞ In 2018, mLQC-I was re-discovered by Dapor and Liegener [PLB785 (2018) 506-510].

2.1a The effective dynamics of mLQC-I

☞ The effective Hamiltonian constraint in mQLC-I takes the form

$$\mathcal{H}_{\rm mLQC-I} = \frac{3v}{8\pi G\lambda^2}\left\{\sin^2(\lambda b) - \frac{(\gamma^2+1)\sin^2(2\lambda b)}{4\gamma^2}\right\} + \mathcal{H}_M.$$

☞ Then, the Friedmann equations can be derived from

$$H^2 = \frac{\sin^2(2\lambda b)}{4\lambda^2\gamma^2}\left\{\gamma^2 - (\gamma^2+1)\cos(2\lambda b)\right\}^2,$$

$$\rho = \frac{3}{8\pi G\lambda^2}\left(-\sin^2(\lambda b) + \frac{(\gamma^2+1)\sin^2(2\lambda b)}{4\gamma^2}\right).$$

or inversely,

$$\sin^2(\lambda b_\pm) = \frac{1 \pm \sqrt{1-\rho/\rho_c^{\rm I}}}{2(\gamma^2+1)},$$

$$\rho_c^{\rm I} = \rho_c/[4(1+\gamma^2)].$$

2.1a The effective dynamics of mLQC-I

☞ More specifically,

$$\sin^2(\lambda b_-) = \begin{cases} 0, & \rho = 0, \\ \frac{1}{2(\gamma^2+1)} \sim 0.47, & \rho = \rho_c^{\mathrm{I}}. \end{cases}$$

In contrast,

$$\sin^2(\lambda b_+) = \begin{cases} \frac{1}{(\gamma^2+1)} \sim 0.95, & \rho = 0, \\ \frac{1}{2(\gamma^2+1)}, & \rho = \rho_c^{\mathrm{I}}. \end{cases}$$

☞ In mLQC-I,

$$\dot{b} = -4\pi G\gamma\dot{\phi}^2 \leq 0.$$

The momentum b has to decrease monotonically. Therefore, the branch b_- alone is not able to cover both the expanding and the contracting phases.

2.1a The effective dynamics of mLQC-I

➢ This figure shows different phases in LQC ($\rho = \rho_c \sin^2(\lambda b)$) [Li and Singh, PRD105, 046013(2022)].

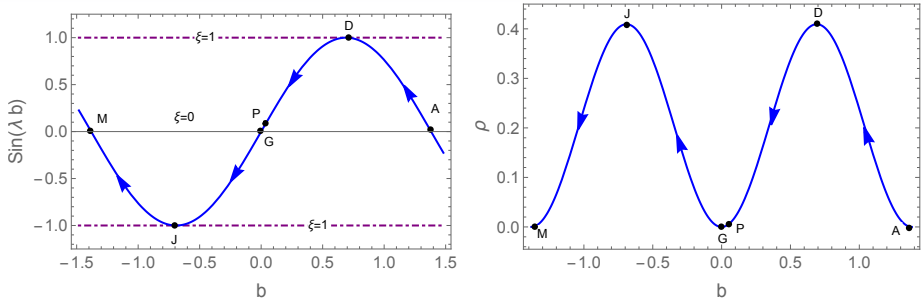

Figure: In the figure, $\sin(\lambda b)$ and ρ are depicted in the forward evolution of the universe in LQC. The arrows denote the direction of time flow. The bounce points are labelled by D, J, and the recollapse points are labelled by A, G, M. ξ stands for the ratio of the energy density of the scalar field over the maximum energy density ρ_c in LQC. Point P which is close to the recollapse point G stands for the macroscopic universe representing the present epoch in this cyclic evolution.

2.1a The effective dynamics of mLQC-I

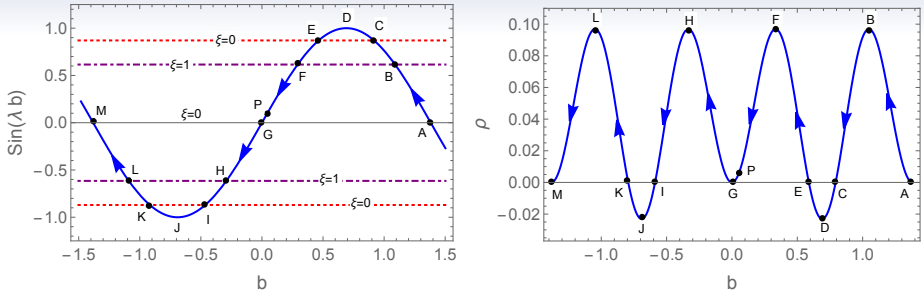

Figure: In the figure, we show the values of $\sin(\lambda b)$ and ρ in mLQC-I when the universe evolves in the direction indicated by the arrows. In the left panel, ξ stands for the ratio of the energy density over the maximum energy density in mLQC-I. Hence, the line $\xi = 0$ corresponds to the moment when the energy density vanishes and the line $\xi = 1$ to the moment when the energy density reaches its maximum. The b_+ branches lie between points $B - F$ and $H - L$, and the rest of trajectory lies in b_- branch. In the right panel, we locate the same bounce and recollapse points in the ρ vs b plot which shows the matter energy density at each corresponding point.

The effective dynamics of mLQC-I

☞ In the b_- branch, we have [Li, Singh and Wang, PRD97, 084029(2018)]

$$H^2 = \frac{8\pi G\rho}{3}\left(1-\frac{\rho}{\rho_c^{\rm I}}\right)\left[1+\frac{\gamma^2}{\gamma^2+1}\left(\frac{\sqrt{\rho/\rho_c^{\rm I}}}{1+\sqrt{1-\rho/\rho_c^{\rm I}}}\right)^2\right],$$

$$\dot{\rho}+3H(\rho+P)=0.$$

☞ In the limit $\rho/\rho_c^{\rm I} \ll 1$, we find

$$H^2 \approx \frac{8\pi G}{3}\rho, \qquad \frac{\ddot{a}}{a} \approx -\frac{4\pi G}{3}(\rho+3P).$$

— GR limit

2.1a The effective dynamics of mLQC-I

☞ In the b_+ branch, we have

$$H^2 = \frac{8\pi G_\alpha \rho_\Lambda}{3}\left(1-\frac{\rho}{\rho_c^{\rm I}}\right)\left[1+\left(\frac{1-2\gamma^2+\sqrt{1-\rho/\rho_c^{\rm I}}}{4\gamma^2\left(1+\sqrt{1-\rho/\rho_c^{\rm I}}\right)}\right)\frac{\rho}{\rho_c^{\rm I}}\right],$$

$$\dot{\rho}+3H(\rho+P)=0,$$

where $G_\alpha \equiv \alpha G = (1-5\gamma^2)G/(1+\gamma^2)$ and $\rho_\Lambda \equiv 3/[8\pi G\alpha\Delta(1+\gamma^2)^2] \simeq \mathcal{O}(\rho_{Pl})$.

☞ In the limit $\rho/\rho_c^{\rm I} \ll 1$, we obtain

$$H^2 \approx \frac{8\pi G_\alpha}{3}(\rho+\rho_\Lambda), \quad \frac{\ddot{a}}{a} \approx -\frac{4\pi G_\alpha}{3}(\rho+3P-2\rho_\Lambda)$$

— GR limit but with a modified G_α and a cosmological constant ρ_Λ

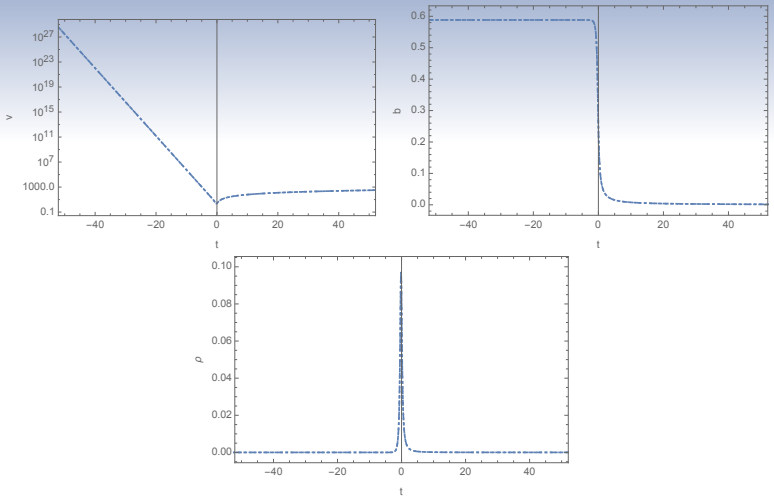

Figure: We compare the numerical results of the Hamilton's equations (dotted line) and the combination of the two branches b_- and b_+ (dot-dashed line). The "initial" data are chosen at $t_0 = 115$ with $\rho_0 = 10^{-6}$, $p_\phi^0 = 1$. The bounce occurs at $t_B = -0.158$. [Li, Singh and Wang, PRD97, 084029(2018)]

2.1b The effective dynamics of mLQC-II

☞ The effective Hamiltonian constraint of mLQC-II takes the form [9],

$$\mathcal{H}_{mLQC-II} = -\frac{3v}{2\pi G\lambda^2\gamma^2}\sin^2\left(\frac{\lambda b}{2}\right)\left\{1+\gamma^2\sin^2\left(\frac{\lambda b}{2}\right)\right\}+\mathcal{H}_M.$$

☞ Similar to mLQC-I,

$$\begin{aligned} H^2 &= \frac{\sin^2(\lambda b)}{\lambda^2\gamma^2}\left\{1+\gamma^2-\gamma^2\cos(\lambda b)\right\}^2, \\ sin^2\left(\lambda b_\pm/2\right) &= \frac{-1\pm\sqrt{1+4\gamma^2\left(\gamma^2+1\right)\rho/\rho_c^{II}}}{2\gamma^2}, \end{aligned}$$

where $\rho_c^{II}\equiv 4(1+\gamma^2)\rho_c$.

☞ Only b_+ is physical!

[9] J. Yang, Y. Ding, Y. Ma, PLB682 (2009) 1.

2.1b The effective dynamics of mLQC-II

☞ For the b_+ branch, we have [10],

$$H^2 = \frac{8\pi G\rho}{3}\left(1+\gamma^2\frac{\rho}{\rho_c}\right)\left(1-\frac{(\gamma^2+1)\rho/\rho_c}{(1+\sqrt{\gamma^2\rho/\rho_c+1})^2}\right),$$
$$\dot{\rho}+3H(\rho+P)=0.$$

☞ In the limit $\rho/\rho_c^{\rm I}\ll 1$, we find

$$H^2 \approx \frac{8\pi G}{3}\rho, \qquad \frac{\ddot{a}}{a}\approx -\frac{4\pi G}{3}(\rho+3P).$$

— GR limit

[10] Li, Singh and Wang, PRD98, 066016(2019).

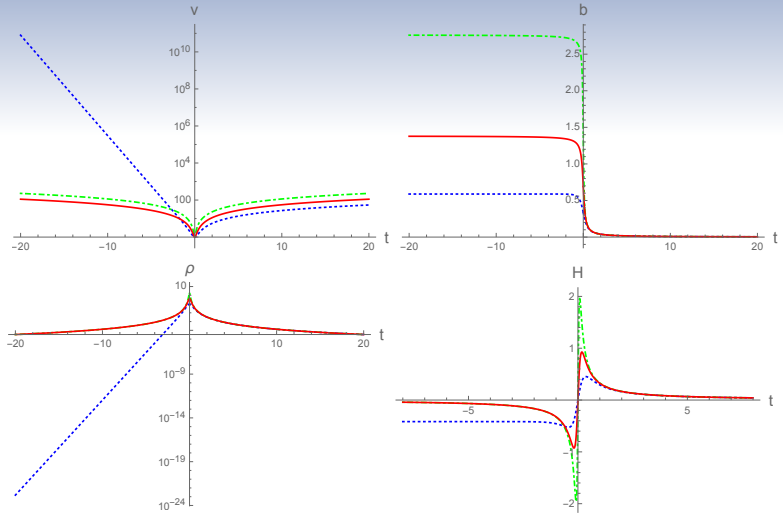

Figure: Comparison of LQC (red solid line), mLQC-I (blue dotted line) and mLQC-II (green dot-dashed line) for a massless scalar field. The initial conditions are chosen at the bounce with ϕ_B set to zero and a positive $\dot{\phi}_B$.

2.2 The inflationary scenario in mLQC

- Embedding the inflationary scenario into LQC requires adding inflationary field(s) to the matter sector, for the most pragmatic purpose, we assume inflation driven by a single scalar field ϕ

$$\mathcal{H}_M = \frac{p_\phi^2}{2v} + vV(\phi).$$

- The background pre-inflationary dynamics in LQC has already been studied extensively[11]). We shall extend such studies to mLQCs, of which we shall study their general properties for inflationary paradigm.

[11] P. Singh, Phys. Rev. D73, 063508 (2006);T. Zhu, A. Wang, G. Cleaver, K. Kirsten and Q. Sheng, Phys. Lett. B773, 196 (2017);Phys. Rev. D97, 043501 (2018);Phys. Rev. D96, 083520 (2017).

2.2 The inflationary scenario in mLQC

- To begin with, we need to define a few physical quantities that can be used to label the different phases of the evolution of the universe.

$$\omega_\phi \equiv \frac{P(t)}{\rho(t)} = \frac{\frac{1}{2}\dot{\phi}^2 - V}{\frac{1}{2}\dot{\phi}^2 + V}.$$

It can take any value in the range of $[-1, 1]$ for a single scalar field with positive potential.

$$\epsilon_H = -\frac{\dot{H}}{H^2}, \quad \epsilon_V = \frac{1}{16\pi G}\left(\frac{V_{,\phi}}{V}\right)^2. \tag{1}$$

The Hubble slow-roll parameter ϵ_H is used in numerical calculations to define precisely when the slow-roll inflation begins and ends.(Note $\ddot{a} = aH^2(1 - \epsilon_H)$) The potential slow-roll parameter ϵ_V is used to determine which part of the potential is able to successfully drive the inflation.

2.2 The inflationary scenario in mLQC

- The number of the inflationary e-foldings is given by

$$N_{inf} = \ln\left(\frac{a_{end}}{a_{on}}\right),$$

where a_{end} represents the scale factor at the end of the inflationary phase, and a_{on} is the scale factor at the onset of inflation.

- For all the numerical calculations, the initial conditions are set at the bounce where

$$\frac{1}{2}\dot{\phi}_B^2 + V(\phi_B) = \rho_c^A,$$

with $A = \mathrm{I}, \mathrm{II}$. At the bounce, $v_B = 1$, $b_B = fixed$. The parameter space is composed of ϕ_B and sign of $\dot{\phi}_B$.

2.2 The inflationary scenario in mLQC

- Here we present some of the results for two representative potentials, the chaotic potential and the Starobinsky potential.
- The chaotic potential

$$V(\phi) = \frac{1}{2} m^2 \phi^2.$$

Three distinct phases can be observed from the bounce point to the end of inflation.

- The bouncing phase where $\omega_\phi \approx 1$.
- The transition phase where ω_ϕ quickly shifts from 1 to -1.
- The inflationary phase where $\omega_\phi \approx -1$.

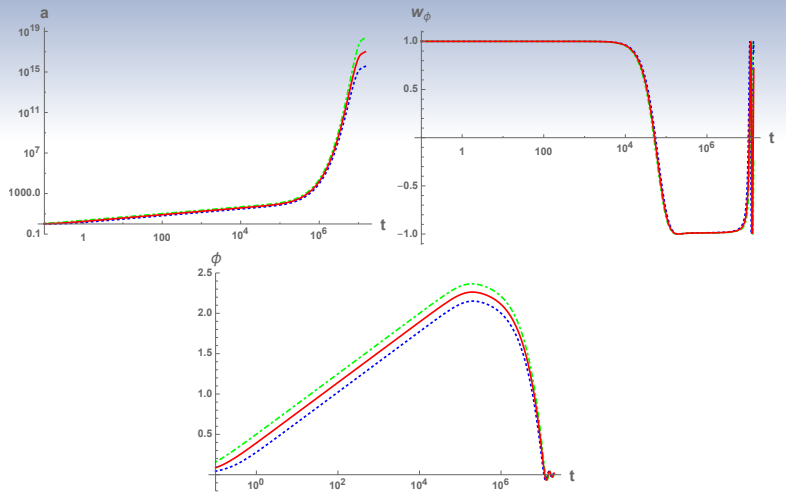

Figure: The evolution of several quantities in the post-bounce phase are depicted and compared: LQC (red solid curves), mLQC-I (blue dotted curves) and mLQC-II (green dot-dashed curves) with the chaotic potential. The initial condition is chosen at the bounce with $\phi_B = 0, \dot{\phi}_B > 0$. The mass of the scalar field is set to $m = 1.26 \times 10^{-6}\ m_{\rm Pl}$.

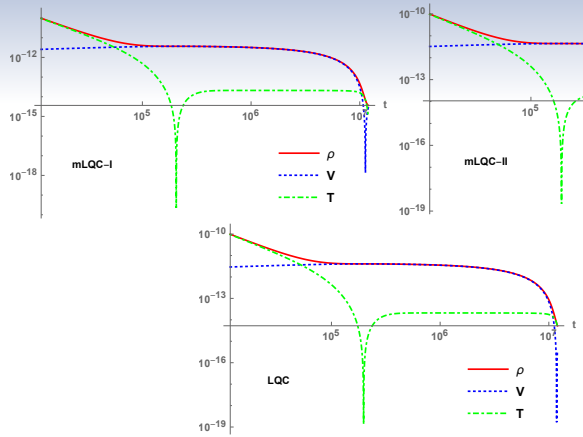

Figure: With the same initial conditions as those in the figure of the above slide, the change in energy density ρ, the KE and PE of the scalar field is shown in each of the three models, LQC, mLQC-I and mLQC-II.

The Starobinsky potential

$$V = \frac{3m^2}{32\pi G}\left(1 - e^{-\sqrt{16\pi G/3}\phi}\right)^2.$$

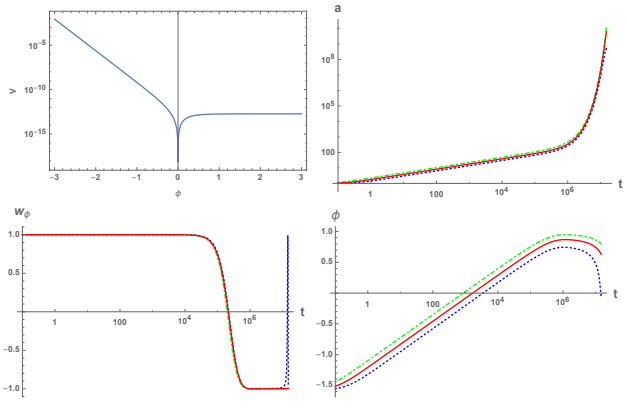

Figure: The initial condition is chosen at the bounce with $\phi_B = -1.6\ m_{\rm Pl}, \dot{\phi}_B > 0$.

Analytical solutions

- As long as the bounce is dominated by the KE, the pre-inflationary evolution of the universe is generic irrespectively of the choice of the potential.
- For both mLQC-I and mLQC-II, the approximate analytical solutions of the background dynamics can be obtained[Li, Singh and Wang, PRD98, 066016(2019).].
  - ✯ Example: The bouncing phase in mLQC-I

$$a(t) = \left[1+24\pi G\rho_{\rm c}^{\rm I}\left(1+\frac{A\gamma^2}{1+Bt}\right)t^2\right]^{1/6},$$

$$\phi(t) = \phi_{\rm B} \pm \frac{m_{\rm Pl}\,\mathrm{arcsinh}\left(\sqrt{24\pi G\rho_{\rm c}^{\rm I}\left(1+\frac{C\gamma^2}{1+Dt}\right)}\,t\right)}{\sqrt{12\pi G\left(1+\frac{C\gamma^2}{1+Dt}\right)}},$$

where the parameters A, B, C and D are fixed through least square method. The best fitting is provided by

$$A = C = 1.2, \quad B = 6, \quad D = 2.$$

Numerical VS Analytical

Table: The analytic and numeric values of several observables are listed in a sequence of events, including Bounce, End of SI (superinflation), Equilibrium point when KE equals PE, the turnaround point when $\dot{\phi} = 0$, the onset of the slow-roll inflation and EOI (end of the inflation).

Event	t_A	t_N	ϕ_A	ϕ_N	$\dot{\phi}_A$	$\dot{\phi}_N$	H_A	H_N	N_A	N_N
Bounce	0	0	0	0	0.440	0.440	0	1.84×10^{-12}	0	0
End of SI	0.364	0.363	0.141	0.141	0.311	0.312	0.452	0.453	0.115	0.114
KE=PE	6.24×10^{4}	5.51×10^{4}	2.07	2.04	2.61×10^{-6}	2.57×10^{-6}	5.35×10^{-6}	7.44×10^{-6}	4.01	4.01
$\dot{\phi} = 0$	2.23×10^{5}	2.05×10^{5}	2.20	2.15	-1.06×10^{-22}	1.14×10^{-23}	5.68×10^{-6}	5.55×10^{-6}	4.91	4.88
Slow-Roll	4.82×10^{5}	4.82×10^{5}	2.16	2.11	-2.11×10^{-7}	-2.03×10^{-7}	5.57×10^{-6}	5.45×10^{-6}	6.37	6.40
EOI	9.63×10^{6}	9.63×10^{6}	0.282	0.201	-2.05×10^{-7}	-1.79×10^{-7}	7.27×10^{-7}	6.36×10^{-7}	35.1	34.7
Bounce	0	0	0.917	0.917	0.440	0.440	0	1.84×10^{-12}	0	0
End of SI	0.364	0.363	1.06	1.06	0.311	0.312	0.452	0.453	0.115	0.114
KE=PE	4.41×10^{4}	3.89×10^{4}	2.93	2.90	3.70×10^{-6}	3.66×10^{-6}	7.56×10^{-6}	1.06×10^{-5}	3.90	3.89
$\dot{\phi} = 0$	1.72×10^{5}	1.59×10^{5}	3.07	3.02	7.94×10^{-23}	-1.23×10^{-23}	7.91×10^{-6}	7.78×10^{-6}	4.90	4.88
Slow-Roll	3.63×10^{5}	3.53×10^{5}	3.04	2.99	-2.10×10^{-7}	-2.03×10^{-7}	7.83×10^{-6}	7.72×10^{-6}	6.41	6.38
EOI	1.38×10^{7}	1.41×10^{7}	0.282	0.201	-2.05×10^{-7}	-1.79×10^{-7}	7.27×10^{-7}	6.36×10^{-7}	63.9	63.0
Bounce	0	0	2.00	2.00	0.440	0.440	0	1.84×10^{-12}	0	0
End of SI	0.364	0.363	2.14	2.14	0.311	0.312	0.452	0.453	0.115	0.114
KE=PE	3.26×10^{4}	2.87×10^{4}	3.97	3.93	5.00×10^{-6}	4.96×10^{-6}	1.02×10^{-5}	1.43×10^{-5}	3.80	3.79
$\dot{\phi} = 0$	1.37×10^{5}	1.27×10^{5}	4.11	4.06	7.94×10^{-23}	4.21×10^{-23}	1.06×10^{-5}	1.04×10^{-5}	4.89	4.87
Slow-Roll	2.82×10^{5}	2.75×10^{5}	4.08	4.03	-2.09×10^{-7}	-2.03×10^{-7}	1.05×10^{-5}	1.04×10^{-5}	6.42	6.41
EOI	1.88×10^{7}	1.92×10^{7}	0.282	0.201	-2.05×10^{-7}	-1.79×10^{-7}	7.27×10^{-7}	6.36×10^{-7}	111	109

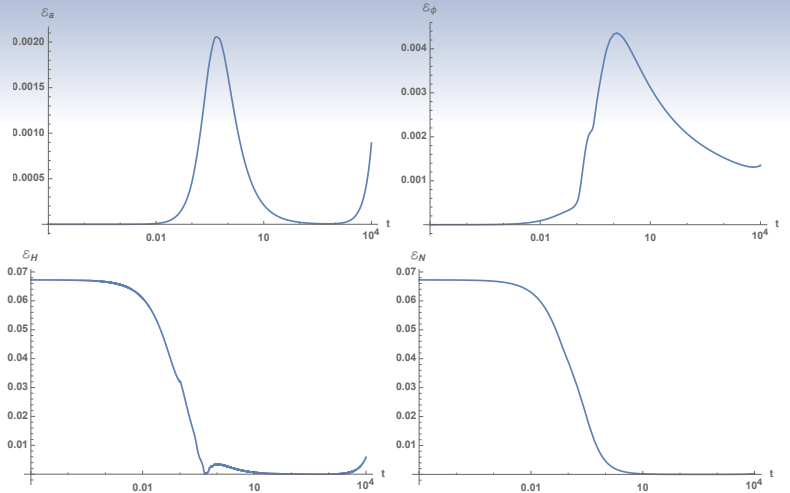

Figure: Relative errors between numerical and analytical solutions for the chaotic potential. The mass of the scalar field is set to 1.26×10^{-6} and the initial conditions are chosen at the bounce with $\phi_B = 0$ and $\dot{\phi}_B > 0$.

The parameter space for the desired slow-roll phase

- In loop cosmological models, there are essentially two "free" parameters: ϕ_B and m. Planck data is required to (partially) fix them.
  - For single field slow-roll inflation, the scalar power spectrum amplitude and the scalar spectral index for the pivot mode $k_* = 0.05\ \mathrm{Mpc}^{-1}$ is given by

$$A_s^* = \frac{8V(\phi_*)}{3\epsilon_V(\phi_*)m_{\mathrm{Pl}}^4}, \quad n_s^* = 1 + 2\eta_V(\phi_*) - 6\epsilon_V(\phi_*),$$

where ϕ_* denotes the value of the scalar field at the moment when the pivot mode exits the horizon during inflation and $\eta_V = \frac{V_{,\phi\phi}}{8\pi GV}$. As a result, the mass of the inflaton and ϕ_* can be found from A_s and n_s.

The parameter space for the desired slow-roll phase

Table: In this table, we list the parameters in the inflationary potentials, the e-folds for the desired slow-roll inflation and the values of the scalar field at the horizon crossing and the end of inflation.

Inflationary Potentials	$V(\phi)$	$\phi_{\mathbf{end}}/m_{\rm Pl}$	$\phi_*/m_{\rm Pl}$	**Parameter**	N_*
Chaotic	$\frac{1}{2}m^2\phi^2$	$\pm\frac{1}{2\sqrt{\pi}} \approx \pm 0.282$	± 3.02	$m = 1.26\times 10^{-6} m_{\rm Pl}$	56.6
Starobinsky	$\frac{3m^2}{32\pi G}\left(1-e^{-\sqrt{\frac{16\pi}{3m_{\rm Pl}^2}}\phi}\right)^2$	$\frac{1}{4}\sqrt{\frac{3}{\pi}}\ln\left(1+\frac{2}{\sqrt{3}}\right) \approx 0.188$	1.07	$m = 2.49\times 10^{-6}\ m_{\rm Pl}$	55.0

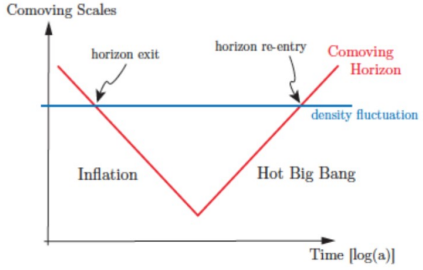

The parameter space for the desired slow-roll phase

- For the desired slow-roll phase, $N_{inf} \geq 56.6$ for the chaotic potential and $N_{inf} \geq 55.0$ for the Starobinsky potential.
  - For the chaotic potential, the range of ϕ_B (with $\dot{\phi}_B > 0$) which allows for at least N_* inflationary e-folds in each model is given by

$$\phi_B^{\rm I} \in (-\phi_{\rm max}^{\rm I}, -5.518\ m_{\rm Pl}) \cup (0.917\ m_{\rm Pl}, \phi_{\rm max}^{\rm I}),$$
$$\phi_B^{\rm II} \in (-\phi_{\rm max}^{\rm II}, -5.386\ m_{\rm Pl}) \cup (0.689\ m_{\rm Pl}, \phi_{\rm max}^{\rm II}),$$

    where $\phi_{\rm max}^{\rm I} = 3.49 \times 10^5\ m_{\rm Pl}, \phi_{\rm max}^{\rm II} = 1.48 \times 10^6\ m_{\rm Pl}$ are the maximum value of ϕ_B in mLQC-I/II.
  - For the Starobinsky potential,

$$\phi_B^{\rm I} \geq -1.349\ m_{\rm Pl}\ \textit{when}\ \dot{\phi}_B^{\rm I} > 0, \phi_B^{\rm I} \geq 3.499\ m_{\rm Pl}\ \textit{when}\ \dot{\phi}_B^{\rm I} < 0$$
$$\phi_B^{\rm II} \geq -1.577\ m_{\rm Pl}\ \textit{when}\ \dot{\phi}_B^{\rm I} > 0, \phi_B^{\rm I} \geq 3.722\ m_{\rm Pl}\ \textit{when}\ \dot{\phi}_B^{\rm I} < 0.$$

The physical measure on the bounce surface

- To consider the probability of the slow-roll inflation in the modified LQC models, the symplectic form on the four-dimensional phase space spanned by v, b from the gravitational sector and ϕ, p_ϕ from the matter sector is

$$\Omega = dp_\phi \wedge d\phi + \frac{dv \wedge db}{4\pi G\gamma}.$$

The vanishing of the effective Hamiltonian constraint reduces the four-dimensional phase space to the hypersurface $\bar{\Gamma}$, on which we have

$$\mathcal{C} = 16\pi G \left\{ \mathcal{H}_{grav}(v, b) + \frac{p_\phi^2}{2v} + vV(\phi) \right\} \simeq 0,$$

where " $\simeq$ " means that the equality holds only on $\bar{\Gamma}$.

The physical measure on the bounce surface

- On the constraint surface, we can solve for the momentum p_ϕ, yielding

$$p_\phi = v\left\{-2\left[\hat{\mathcal{H}}_{grav} + V(\phi)\right]\right\}^{1/2},$$

with

$$\hat{\mathcal{H}}^{\rm A}_{grav} \equiv v^{-1}\mathcal{H}^{\rm A}_{grav}(v, b_0).$$

- Then on the bounce surface with the gauge fixing condition $b = b_B$, from the expression of p_ϕ, we can find

$$dp_\phi = \frac{p_\phi}{v}dv - \frac{v^2 V_{,\phi}}{p_\phi}d\phi.$$

- This can lead to the Liouville measure $d\hat{\mu}_L$ on the bounce surface

$$d\hat{\mu}^{\rm A}_L = \left\{-2\left[\hat{\mathcal{H}}^{\rm A}_{grav}(b_B) + V(\phi)\right]\right\}^{1/2} d\phi dv.$$

The physical measure on the bounce surface

- Since the rescaling of v amounts to a gauge transformation and the Liouville measure does not depend on the volume, we can simply drop dv, arriving at the measure for the space of physically distinct solutions

$$d\omega = \left\{-2\left[\hat{\mathcal{H}}_{grav}(b_B) + V(\phi)\right]\right\}^{1/2} d\phi = (2\rho_c - 2V)^{\frac{1}{2}}\, d\phi.$$

- With this measure and the allowed range of the inflaton field for the desired slow-roll inflation, we can compute the probability of slow-roll inflation for the chaotic inflation [12].

[12] A. Ashtekar and D. Sloan, Gen. Relativ. Gravit. 43, 3619 (2011)

The probability of slow-roll inflation in mLQCs

➥ For mLQC-I and mLQC-II, we can employ the same form of the physical measure as long as the maximum energy density is replaced by the one in each model.

✯ Specifically, the probability for the desired slow-roll not to happen is

$$P^{\rm I}(\text{not realized}) \lesssim \frac{\int_{-5.158}^{0.917} d\omega^{\rm I}}{\int_{-\phi^{\rm I}_{\rm max}}^{\phi^{\rm I}_{\rm max}} d\omega^{\rm I}} \simeq 1.12 \times 10^{-5},$$

where $\phi^{\rm I}_{\rm max}$ is the maximum value of the inflaton field allowed for the chaotic potential.

✯ The probability for the desired slow-roll not to happen in mLQC-II is

$$P^{\rm II}(\text{not realized}) \lesssim 2.62 \times 10^{-6}.$$

✯ The probability for desired slow roll inflation not to occur in LQC is

$$P^{\rm LQC}(\text{not realized}) \lesssim 2.74 \times 10^{-6}.$$

2.2a The Qualitative Dynamics

- Qualitative dynamics[13] plays an important role to visualize the collective behavior of the solutions of the dynamical system.
- In the cosmological settings, the phase space portraits are usually used to identify the slow-roll inflationary separatrices as well as the fixed points of the dynamical systems.
- In LQC, qualitative dynamics has been already studied for several potentials, including chaotic, Starobinsky, and α-attractor[P. Singh and K. Vandersloot, PRD**72**, 084004 (2005);E. Ranken, P. Singh, PRD85, 104002 (2012);A.Ashtekar and D. Sloan, GRG**43**, 3619 (2011);A. Corichi and A. Karami,PRD**83**, 104006 (2011);I. Agullo, A. Ashtekar and W. Nelson,CQG**30**, 085014 (2013);B. Bonga and B. Gupt, PRD93, 063513 (2016); T. Zhu, A.W, G. Cleaver, K. Kirsten and Q. Sheng, PLB**773**, 196 (2017); PRD96, 083520 (2017); M. Shahalam, M. Sharma, Q. Wu, A.W, PRD96, 123533 (2017)].

[13] Oleg I. Bogoyavlensky, Methods in the Qualitative Theory of Dynamical Systems in Astrophysics and Gas Dynamics, Springer-Verlag Berlin Heidelberg, 1985.

2.2a The Qualitative Dynamics

- The qualitative dynamics of mLQC-I/II is studied in the cases of the chaotic, Starobinsky, monodromy, non-minimal Higgs, and exponential potentials [14].
- In the following I shall only talk about the results of the chaotic potential for the pedagogical purpose.

[14] B.-F. Li, P. Singh, A. W, Phys. Rev. D98, 066016.

2.2a The Qualitative Dynamics

- To analyze the qualitative dynamics, the system under study should be converted into an autonomous system which is described by a set of first-order equations (usually n-dimensional)

$$\begin{aligned} \dot{X} &= f(X, Y), \\ \dot{Y} &= g(X, Y). \end{aligned}$$

- The fixed point (X_0, Y_0) is one of the solutions of the system which satisfies

$$\begin{aligned} f(X_0, Y_0) = 0, \\ g(X_0, Y_0) = 0. \end{aligned}$$

- One important object that determines the stability of the fixed point (X_0, Y_0) is the Jacobian matrix evaluated at (X_0, Y_0) which is defined by

$$J = \begin{vmatrix} \partial_{X_0} f & \partial_{Y_0} f \\ \partial_{X_0} g & \partial_{X_0} g \end{vmatrix},$$

2.2a The Qualitative Dynamics

- If the real parts of all the eigenvalues of J are negative, then the fixed point is locally stable.
- If the real part of at least one of the eigenvalues of J is positive, then the fixed point is locally unstable.
- The fixed points whose stability can be determined from the above criteria are called simple fixed points.

2.2a The Qualitative Dynamics

- In mLQCs, there are four phase space variables v, b, ϕ and p_ϕ, among which the inflationary phase is directly related with the latter two variables.
  - ✯ Converting the Klein-Gordon equation $\ddot{\phi} + 3H\dot{\phi} + V_{,\phi} = 0$, into a set of two first-order ODEs. In the chaotic potential, we define

$$X = \frac{m\phi}{\sqrt{2\rho_c^A}} \qquad Y = \frac{\dot{\phi}}{\sqrt{2\rho_c^A}},$$

leading to

$$\dot{X} = mY, \ \dot{Y} = -mX - 3HY.$$

  - ✯ The fixed point locates at $(X, Y) = (0, 0)$.
  - ✯ At the bounce point, $X^2 + Y^2 = 1$.

2.2a The Qualitative Dynamics

- In LQC, mLQC-II and the expanding phase of mLQC-I, the eigenvalues of the Jacobian matrix at $(X = 0, Y = 0)$ are $\pm im$.
- In the contracting phase of mLQC-I, the eigenvalues of the Jacobian matrix at $(X = 0, Y = 0)$ are

$$J_{\pm} = \frac{1}{2\lambda(1+\gamma^2)}\left(3 \pm \sqrt{9 - 4m^2\lambda^2(1+\gamma^2)^2}\right).$$

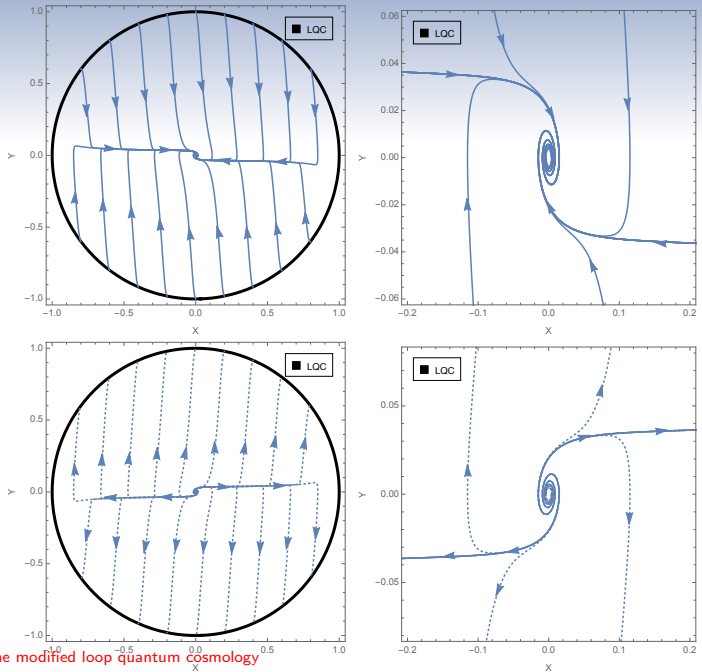
LQC
X
Y
LQC
X
Y
LQC
X
Y
LQC
X
Y

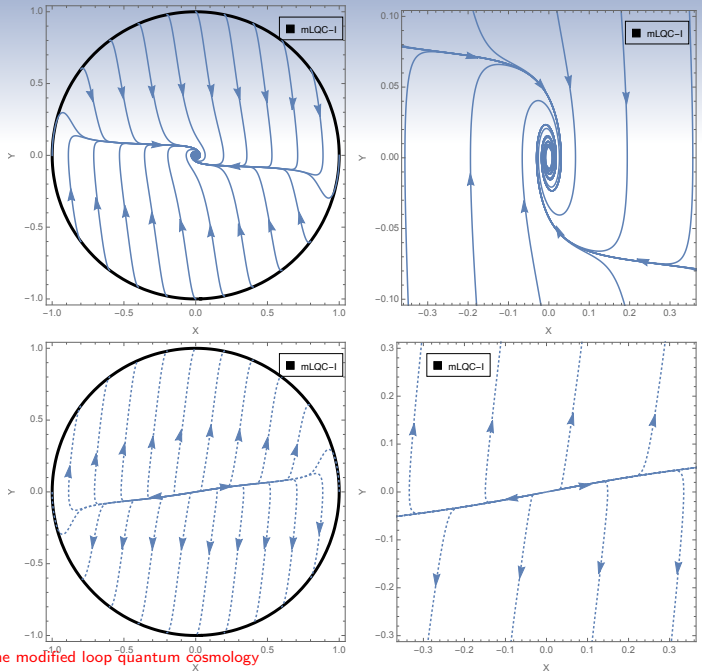
mLQC−I
X
Y
1.0
0.5
0.0
−0.5
−1.0
mLQC−I
X
Y
0.10
0.05
0.00
−0.05
−0.10
−0.3
−0.2
−0.1
0.0
0.1
0.2
0.3
mLQC−I
X
Y
mLQC−I
X
Y
0.3
0.2
0.1
0.0
−0.1
−0.2
−0.3

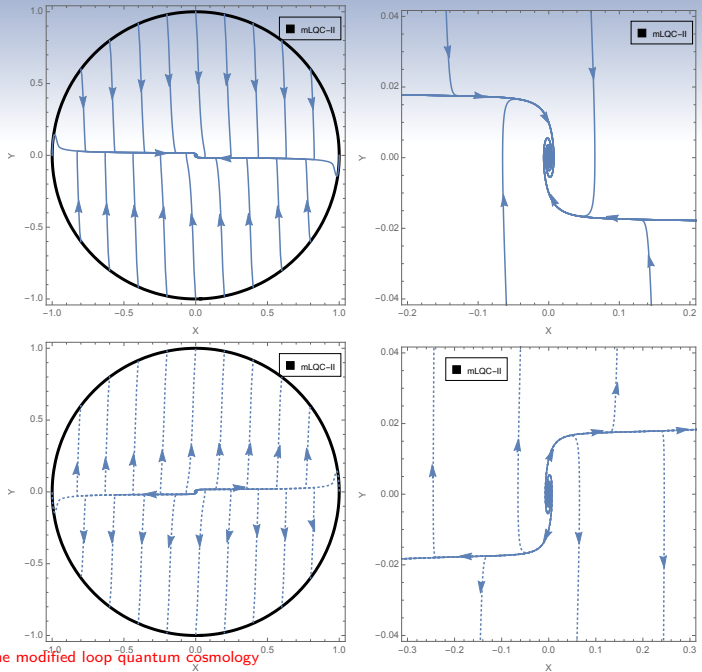
mLQC-II
mLQC-II
mLQC-II
mLQC-II
X
Y

3. The linear perturbations in the modified loop quantum cosmology

3.1 The dressed metric and the hybrid approaches

- In standard LQC, the evolution of the cosmological linear perturbations on the quantum background spacetime has been extensively investigated in four approaches:
  - The dressed metric approach [Agullo, Ashtekar, Nelson, PRL109, 251301 (2012); PRD87,043507 (2013); Class. Quant. Grav. 30,085014 (2013)]
  - The hybrid approach [Gomar, et al, PRD90,064015 (2014); JCAP 1506, 045 (2015); PRD96, 103528 (2017)]
  - The deformed algebra approach [Bojowald, et al, PRD78,063547 (2008); Cailleteau, et al, PRD86,087301 (2012); Class. Quant. Grav 29, 095010 (2012); PRD96, 103528 (2017)]
  - The separate universe approach [Wilson-Ewing, Int. J. Mod. Phys. D25, 1642002 (2016)]
- The dressed metric and the hybrid approaches have been extended to mLQC-I/II [I. Agullo, Gen. Rel. Grav. 50 (2018) 91; Li, Olmedo, Singh, Wang,PRD102, 126025 (2020); Li,Singh,Wang, PRD101, 086004 (2020);B. E. Navascués and G. A. M. Marugán, Class. Quant. Grav. 39, no.1, 015017 (2022).] .

General view: the dressed metric approach v.s. the hybrid approach

- Similarities of two approaches
  - Based on the classical formulation of the perturbation theory. The dressed metric approach is based on the work by Langlois [Class. Quant. Grav. 11,389 (1994)] while the hybrid approach on the seminal work by Halliwell and Hawking [PRD31, 1777(1985)].
  - The background is polymer quantized while the linear perturbations are Fock quantized.
  - Practically, the backreaction of the linear perturbations is ignored and we make use of the test-field approximation so that the effective dynamics in LQC is valid.

General view: the dressed metric approach v.s. the hybrid approach

- Major differences of two approaches [15]
  - Fock quantization of the linear perturbations is implemented with respect to different gauge invariant variables:
    The dressed metric approach: Mukhanov-Sasaki variable $Q_{\vec{k}}$
    The hybrid approach: the rescaled variable $\nu_{\vec{k}} = aQ_{\vec{k}}$
  - Different forms of the classical mass function which appears in the Mukhanov-Sasaki equation

$$\nu''_{\vec{k}} + \left(k^2 + m^2\right)\nu_{\vec{k}} = 0,$$

    are polymerized.

[15] B.-F. Li, P. Singh, Phys. Rev. D106, 086015.

Linear perturbation theory in the Hamiltonian formulation

- Consider a spatially flat homogeneous and isotropic FLRW universe filled with a scalar field.
- In ADM decomposition, a 4-dimensional manifold $\mathcal{M}$ can be decomposed into $\mathcal{M} := \Sigma \times \mathbb{R}$, where Σ is the spacelike hypersurface and $\mathbb{R}$ denotes the real line. Correspondingly, the 4-metric $g_{\mu\nu}$ can be expressed in terms of the lapse N, the shift N^i and the 3-metric γ_{ij}.
- Following Langlois' approach, the lapse and the shift are treated as the Lagrange multipliers. Then the classical phase space is composed of $\Gamma=\{\gamma_{ij}, \pi^{ij}, \Phi, \pi_\Phi\}$ and the total action can then be written in the form

$$S = \int d^4x \left(\pi_\Phi \dot{\Phi} + \pi^{ij}\dot{\gamma}_{ij} - N\mathcal{H} - N^i\mathcal{H}_i\right).$$

Linear perturbation theory in the Hamiltonian formulation

- In the above action, the scalar and the vector constraints are given by

$$\begin{aligned}\mathcal{H} &= \frac{2\kappa}{\sqrt{\gamma}}\left(\pi^{ij}\pi_{ij}-\frac{\pi^2}{2}\right)-\frac{\sqrt{\gamma}}{2\kappa}{}^{(3)}R+\frac{\pi_\Phi^2}{2\sqrt{\gamma}}\\ &+ \sqrt{\gamma}U+\frac{\sqrt{\gamma}}{2}\partial_i\Phi\partial^i\Phi,\\ \mathcal{H}_i &= -2\partial_j\left(\gamma_{ik}\pi^{kj}\right)+\pi^{jk}\partial_i\gamma_{jk}+\pi_\Phi\partial_i\Phi.\end{aligned}$$

- With the decomposition of the phase space variables into the homogeneous sector plus the inhomogeneous perturbations,

$$\begin{aligned}\Phi &= \bar{\phi}(t)+\delta\phi(t,\vec{x}),\quad \pi_\Phi=\bar{\pi}_\phi(t)+\delta\pi_\phi(t,\vec{x}),\\ \gamma_{ij} &= \bar{\gamma}_{ij}(t)+\delta\gamma_{ij}(t,\vec{x}),\pi^{ij}=\bar{\pi}^{ij}(t)+\delta\pi^{ij}(t,\vec{x}).\end{aligned}$$

Linear perturbation theory in the Hamiltonian formulation

- The scalar and the vector constraints can be expanded in the ascending powers of the perturbations. Up to the second order in perturbations, they can be written as

$$\mathcal{H} = \mathcal{H}^{(0)} + \mathcal{H}^{(1)} + \mathcal{H}^{(2)}, \qquad \mathcal{H}_i = \mathcal{H}_i^{(1)} + \mathcal{H}_i^{(2)}.$$

- Considering the simplest cosmological setting—the spatially flat homogeneous and isotropic FLRW background, the zeroth-order Hamiltonian constraint is given by

$$\mathcal{H}^{(0)} = -\frac{\kappa \pi_a^2}{12a} + \frac{\bar{\pi}_\phi^2}{2a^3} + a^3 U,$$

where we used $\bar{\gamma}_{ij} = a^2 \delta_{ij}$ and $\bar{\pi}^{ij} = \pi_a \delta^{ij}/6a$ with $\pi_a = -6Ha^2/(N\kappa)$.

Linear perturbation theory in the Hamiltonian formulation

- At the zeroth order,

$$H_0 = \int d^3x\, N\mathcal{H}^{(0)} = NV_0\left(-\frac{\kappa\pi_a^2}{12a} + \frac{\bar{\pi}_\phi^2}{2a^3} + a^3U\right).$$

- Now using the relations

$$v = V_0a^3,\ p_\phi = \bar{\pi}_\phi V_0,\ \pi_a = \frac{-6c|p|^{1/2}}{\gamma\kappa V_0^{2/3}},$$

we can recover the classical background Hamiltonian constraint

$$H_0 = -\frac{3vb^2}{8\pi G\gamma^2} + \frac{p_\phi^2}{2v} + vU(\phi).$$

Linear perturbation theory in the Hamiltonian formulation

- Next, we need to deal with the first-order scalar constraint $\mathcal{H}^{(1)}$ and first-order vector constraint $\mathcal{H}_i^{(1)}$.
- To proceed, it is more convenient to work in the momentum space in which linear perturbations are expanded in terms of the Fourier series as for instance

$$\delta\phi(t,\vec{x}) = \sum_{\vec{k}} \delta\phi_{\vec{k}}(t) e^{i\vec{k}\cdot\vec{x}},$$

with its Fourier coefficients given by

$$\delta\phi_{\vec{k}}(t) = \frac{1}{V_o}\int d^3x \delta\phi(t,\vec{x}) e^{-i\vec{k}\cdot\vec{x}}.$$

Linear perturbation theory in the Hamiltonian formulation

- For the metric perturbations $\delta\gamma_{ij}$ and their conjugate momenta $\delta\pi^{ij}$, one can introduce six orthonormal bases A^m_{ij} with $m = 1, 2...6$. In term of these bases, we can separate different modes as

$$\delta\gamma_{ij} = \gamma_m A^m_{ij}, \qquad \delta\pi^{ij} = \pi^m A^{ij}_m,$$

where γ_1, γ_2 are the scalar modes, γ_3, γ_4 are the vector modes and γ_5, γ_6 the tensor modes.

$$A^1_{ij} = \frac{1}{\sqrt{3}}\bar{\gamma}_{ij},\ A^2_{ij} = \sqrt{\frac{3}{2}}\left(\hat{k}_i\hat{k}_j - \frac{\bar{\gamma}_{ij}}{3}\right),\ A^3_{ij} = \sqrt{\frac{1}{2}}\left(\hat{k}_i\hat{x}_j + \hat{k}_j\hat{x}_i\right),$$
$$A^4_{ij} = \sqrt{\frac{1}{2}}\left(\hat{k}_i\hat{y}_j + \hat{y}_j\hat{k}_i\right),\ A^5_{ij} = \sqrt{\frac{1}{2}}\left(\hat{x}_i\hat{x}_j - \hat{y}_i\hat{y}_j\right),\ A^6_{ij} = \sqrt{\frac{1}{2}}\left(\hat{x}_i\hat{y}_j + \hat{x}_j\hat{y}_i\right).$$

Linear perturbation theory in the Hamiltonian formulation

- Now we can express the first-order scalar constraint in terms of the scalar modes and the perturbations in the scalar field $\delta\phi$ and its momentum $\delta\pi_\phi$, it turns out

$$\mathcal{H}^{(1)} = f(\gamma_1, \gamma_2, \pi^1, \delta\phi, \delta\pi_\phi) = 0.$$

- Regarding the first-order vector constraint $\mathcal{H}_i^{(1)}$, we have
  - $k^i\mathcal{H}_i^{(1)} = g(\gamma_1, \gamma_2, \pi^1, \pi^2, \delta\phi) = 0$,
  - $x^i\mathcal{H}_i^{(1)} = f_1(\gamma_3, \pi^3) = 0$,
  - $y^i\mathcal{H}_i^{(1)} = f_2(\gamma_4, \pi^4) = 0$.
- Counting the degrees of freedom in configuration space:
  Scalar modes: 3; Vector modes: 2; Tensor modes: 2.
  Number of constraints: 4
  Physical degrees of freedom:3= 1 scalar mode +2 tensor modes

Linear perturbation theory in the Hamiltonian formulation

- $\mathcal{H}^{(1)}$ and the longitudinal part of $\mathcal{H}_i^{(1)}$ constrain the scalar modes while the transverse part of $\mathcal{H}_i^{(1)}$ constrain the vector modes.
- To proceed, two possible approaches:
  1. Choosing a particular gauge (dressed metric approach, hybrid approach) and then working in the reduced phase space
  2. Constructing gauge-invariant variables and finding their second-order Hamiltonian (hybrid approach)

Linear perturbation theory in the Hamiltonian formulation

- Here we adopt the first approach—choosing the spatially flat gauge, $\gamma_1 = \gamma_2 = 0$. Combining with $\mathcal{H}^{(1)} = k^i \mathcal{H}_i^{(1)} = 0$, leaving only $\delta\phi_{\vec{k}}$, its second-order Hamiltonian [16]

$$\mathbf{H}^{(2)} = NV_o \sum_{\vec{k}^+} \mathcal{H}^{(2)}_{\rm SF},$$

with

$$\mathcal{H}^{(2)}_{\rm SF} = \frac{|\delta\pi_{\phi_{\vec{k}}}|^2}{a^3} - \frac{3\bar{\pi}_\phi^2}{\pi_a a^4}\left(\delta\phi_{\vec{k}}\delta\pi_{\phi_{-\vec{k}}} + \delta\phi_{-\vec{k}}\delta\pi_{\phi_{\vec{k}}}\right) + \aleph|\delta\phi_{\vec{k}}|^2,$$

and

$$\aleph = ak^2 + \frac{3\kappa\bar{\pi}_\phi^2}{2a^3} - 6a^2 U_{,\bar{\phi}}\frac{\bar{\pi}_\phi}{\pi_a} + a^3 U_{,\bar{\phi}\bar{\phi}}.$$

[16] Li,Singh, PRD106, 086015 (2022).

Linear perturbation theory in the Hamiltonian formulation

- Next we need to remove the cross terms in the second-order Hamiltonian constraint, to achieve this, we use the new variables

$$Q_{\vec{k}} = \delta\phi_{\vec{k}}, \qquad P_{Q_{\vec{k}}} = \delta\pi_{\phi_{\vec{k}}} - \frac{3\bar{\pi}_\phi^2}{a\pi_a}\delta\phi_{\vec{k}}.$$

The corresponding second-order Hamiltonian takes the form

$$\tilde{\mathcal{H}}^{(2)} = \frac{|P_{Q_{\vec{k}}}|^2}{a^3} + a\left(k^2 + \Omega^2\right)|Q_{\vec{k}}|^2,$$

with

$$\Omega^2 = \frac{3\kappa\bar{\pi}_\phi^2}{a^4} - 18\frac{\bar{\pi}_\phi^4}{\pi_a^2 a^6} - 12a\frac{\bar{\pi}_\phi U_{,\bar{\phi}}}{\pi_a} + a^2 U_{,\bar{\phi}\bar{\phi}},$$

leading to the Mukhanov-Sasaki (MS) equation

$$\ddot{Q}_{\vec{k}} + 3H\dot{Q}_{\vec{k}} + \frac{k^2 + \Omega^2}{a^2}Q_{\vec{k}} = 0.$$

Linear perturbation theory in the Hamiltonian formulation

- In order to remove the first-order derivative term, one can define $\nu_{\vec{k}} = aQ_{\vec{k}}$, resulting in the alternative form of MS equation

$$\nu_{\vec{k}}'' + \left(k^2 + \Omega^2 - \frac{a''}{a}\right)\nu_{\vec{k}} = 0,$$

where we define the classical mass function

$$m_{\mathrm{SF}}^2 = \Omega^2 - \frac{a''}{a}.$$

It is the mass squared of the Harmonic oscillator when m_{SF}^2 is time-independent.

Linear perturbation theory in the Hamiltonian formulation

- On the other hand, one can directly use the rescaled variable by requiring

$$\nu_{\vec{k}} = a\delta\phi_{\vec{k}}, \qquad \pi_{\nu_{\vec{k}}} = \frac{\delta\pi_{\phi_{\vec{k}}}}{a} - \frac{3\bar{\pi}_{\phi}^2}{\pi_a a^2}\delta\phi_{\vec{k}} - \frac{a}{6}\kappa\pi_a\delta\phi_{\vec{k}}.$$

- The corresponding second-order Hamiltonian takes the form

$$\tilde{\mathcal{H}}^{(2)} = \frac{|\pi_{\nu_{\vec{k}}}|^2}{a} + \frac{1}{a}\left(k^2 + \tilde{m}_{\rm SF}^2\right)|\nu_{\vec{k}}|^2,$$

where the classical mass function is given by

$$\tilde{m}_{\rm SF}^2 = -\frac{27\bar{\pi}_{\phi}^4}{2\pi_a^2 a^6} + \frac{5\kappa\bar{\pi}_{\phi}^2}{2a^4} + \frac{9\bar{\pi}_{\phi}^2 U}{\pi_a^2} - 12aU_{,\bar{\phi}}\frac{\bar{\pi}_{\phi}}{\pi_a} - \frac{\kappa^2\pi_a^2}{72a^2} + a^2U_{,\bar{\phi}\bar{\phi}} - \frac{\kappa}{2}a^2U.$$

Linear perturbation theory in the Hamiltonian formulation

- In the classical theory, all the above analyses converge to the same mass function in the Mukhanov-Sasaki equation of $\nu_{\tilde{k}}$ on the classical trajectories of the Friedmann dynamics since the difference between two forms of the mass function turns out to be

$$\delta m^2_{\rm SF} = m^2_{\rm SF} - \tilde{m}^2_{\rm SF} = -\left(\frac{9\bar{\pi}^2_\phi}{a^3\pi^2_a} + \frac{\kappa}{6a}\right)\mathcal{H}^{(0)} \approx 0.$$

- The classical mass functions resulting from other gauges are also equivalent to the one in the spatially flat gauge when the background constraint is satisfied.

Polymerization of the classical mass functions in LQC

- Next we discuss the polymerization of the classical mass function when the effective dynamics is valid. Under this assumption, in the classical mass functions, only $1/\pi_a^2$ and $1/\pi_a$ need to be polymerized.
- Consistent with the polymerization of the background dynamics, we require

$$\frac{1}{\pi_a^2} = \frac{\kappa^2\gamma^2}{36a^4b^2} \to \frac{\kappa^2\gamma^2\lambda^2}{36v^{4/3}\sin^2(\lambda b)} = \frac{\kappa}{12v^{4/3}\rho},$$

  where $b = c/|p|^{1/2}$.
- While for $1/\pi_a$, we require

$$\frac{1}{\pi_a} = -\frac{\kappa\gamma}{6a^2b} \to -\frac{\kappa\gamma\lambda\cos(\lambda b)}{6a^2\sin(\lambda b)} = -\frac{H}{2v^{2/3}\rho}.$$

The effective mass functions in LQC

- The effective mass function in the dressed metric approach takes the form

$$m^2_{\rm eff} = -\frac{4\pi G}{3}a^2\rho\left(1+2\frac{\rho}{\rho_c}\right)+4\pi G a^2 P\left(1-2\frac{\rho}{\rho_c}\right)+\mathfrak{U},$$

- The effective mass function in the hybrid approach reads

$$\tilde{m}^2_{\rm eff} = -\frac{4\pi G}{3}a^2\left(\rho-3P\right)+\mathfrak{U},$$

with

$$\mathfrak{U} = a^2\left(U_{,\bar{\phi}\bar{\phi}}+48\pi G U+6H\frac{\dot{\bar{\phi}}}{\rho}U_{,\bar{\phi}}-\frac{48\pi G}{\rho}U^2\right).$$

and U stands for the potential of the scalar field.

The effective mass functions in mLQCs

- It is then straightforward to extend the dressed metric approach in LQC to mLQC-I and mLQC-II.
- mLQC-I: $b_{\rm I}^2 \to -\frac{\gamma^2}{\lambda^2}\left\{\sin^2(\lambda b) - \frac{\gamma^2+1}{4\gamma^2}\sin^2(2\lambda b)\right\} \to \frac{1}{\pi_a^{\rm I\,2}} = \frac{64\pi^2 G^2\gamma^2\lambda^2}{9a^4\left((1+\gamma^2)\sin^2(2\lambda b) - 4\gamma^2\sin^2(\lambda b)\right)}$
- mLQC-II: $b_{\rm II}^2 \to \frac{4}{\lambda^2}\sin^2\left(\frac{\lambda b}{2}\right)\left\{1+\gamma^2\sin^2\left(\frac{\lambda b}{2}\right)\right\} \to \frac{1}{\pi_a^{\rm II\,2}} = \frac{4\pi^2\gamma^2\lambda^2}{9a^4\sin^2(\lambda b/2)(1+\gamma^2\sin^2(\lambda b/2))}$
- mLQC-I: $\frac{1}{\pi_a^{\rm I}} = \frac{8\pi G\gamma\lambda\tilde{\Theta}(b)}{3a^2\sqrt{(1+\gamma^2)\sin^2(2\lambda b) - 4\gamma^2\sin^2(\lambda b)}}$, with $\tilde{\Theta}(b) = 1 - 2(1+\gamma^2)\sin^2(\lambda b)$.
- mLQC-II: $\frac{1}{\pi_a^{\rm II}} = -\frac{2\pi\gamma\lambda\cos(\lambda b/2)}{3a^2\sin(\lambda b/2)\sqrt{1+\gamma^2\sin^2(\lambda b/2)}}$.

3.2 Matching with CMB

- In the dressed metric and the hybrid approaches in LQC and mLQCs, the linear perturbations obey the MS equation

$$\nu_{\vec{k}}'' + \left(k^2 + m_{\rm eff}^2\right)\nu_{\vec{k}} = 0.$$

- The comoving curvature perturbation observed from CMB can be computed from

$$P_{\mathcal{R}_k} = \frac{k^3}{2\pi^2}\frac{|\nu_k|^2}{z_s^2},$$

where $z_s = a\dot{\phi}/H$ and all the relevant quantities are evaluated at the end of inflation.

- Therefore, the MS equation should be evolved from some initial time to the end of inflation. The choice of the initial states is a long-standing problem since loop cosmological models have a contracting phase beyond the bounce point, we choose the initial state in the distant past of the contracting phase when all the relevant modes are inside the Hubble horizon.

3.2 Matching with CMB

☞ The initial states can be chosen as the adiabatic states, which are essentially the WKB solutions of the MS equation, which reads

$$\nu_k = \frac{1}{\sqrt{2W_k}} e^{-i\int^\eta W_k(\bar{\eta})d\bar{\eta}}.$$

Plugging the above solution back into the MS equation, we have

$$W_k^2 = k^2 + m_{eff}^2 - \frac{1}{2}\frac{W_k''}{W_k} + \frac{3}{4}\left(\frac{W_k'}{W_k}\right)^2.$$

This generates a series of the adiabatic states, starting with the zeroth-order $W_k^{(0)} = k$ and succeeded by the second-order $W_k^{(2)} = \sqrt{k^2 + m^2}$, the fourth-order $W_k^{(4)} = \frac{\sqrt{f(m_{eff}^2, k)}}{4|k^2+s|}$, and so on.
$f(s,k) = 5s'^2 + 16k^4(k^2+3s) + 16s^2(3k^2+s) - 4s''(k^2+s)$.

3.2 Matching with CMB

- For the background dynamics, we choose the Starobinsky potential as the inflationary potential

$$U(\phi) = \frac{m^2}{32\pi G}\left(1 - e^{-\sqrt{\frac{16\pi G}{3}}\phi}\right)^2.$$

- Choosing $m = 2.7 \times 10^{-6}$ and $N_{inf} = 65$ in LQC and mLQC-I/II [17].

[17] Li, Motaharfar and Singh, PRD110, 066005 (2024).

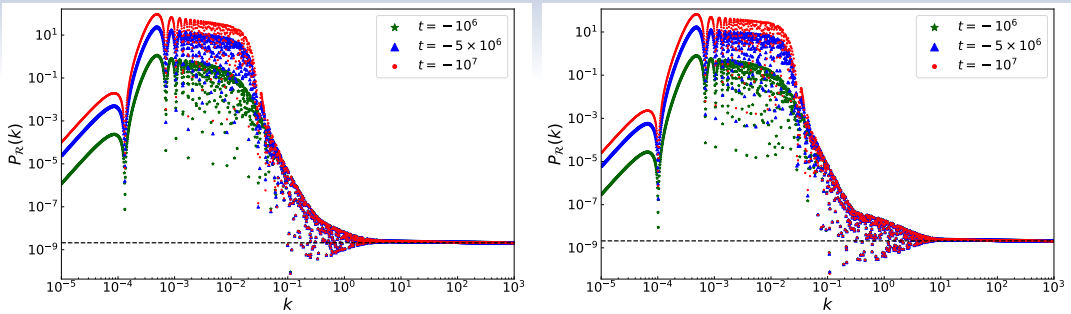

Figure: The primordial power spectrum for LQC with $\phi_B = -1.4306$ and $m = 2.7 \times 10^{-6}$, while second order adiabatic initial states are imposed at $t = -10^6$, -5×10^6, and -10^7 for the hybrid (left) and the dressed metric (right) approaches (all in Planck units).The dashed line is the central value for the amplitude of the primordial power spectrum, i.e., $A_s = 2.0989 \times 10^{-9}$ at pivot scale $k_\star/a_0 = 0.05\mathrm{Mpc}^{-1}$.

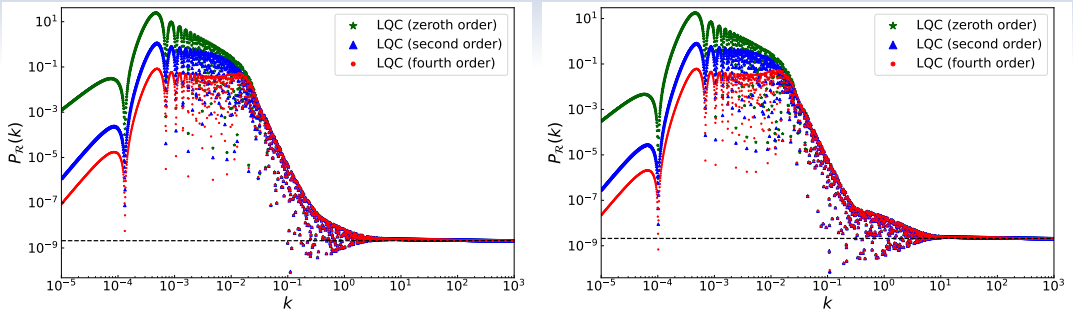

Figure: The primordial power spectrum for LQC with different adiabatic initial states (zeroth, second, and fourth order) in the hybrid approach (left panel) and the dressed metric (right panel) approach, while $t = -10^6$, $\phi_B = -1.4306$, and $m = 2.7 \times 10^{-6}$ (all in Planck units).

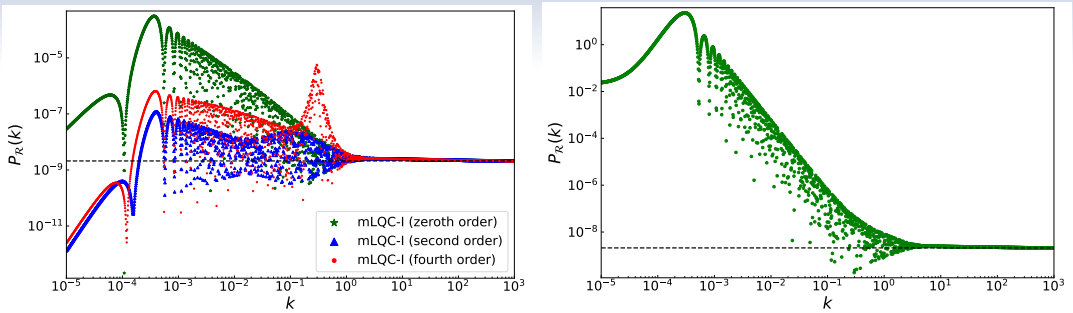

Figure: The primordial power spectrum for mLQC-I with different adiabatic initial states (zeroth, second, and fourth order) in the hybrid approach (left) and with the de Sitter initial state in the dressed metric approach (right) while $t = -2.4$, $\phi_B = -1.31$ and $m = 2.7 \times 10^{-6}$ (in Planck units).

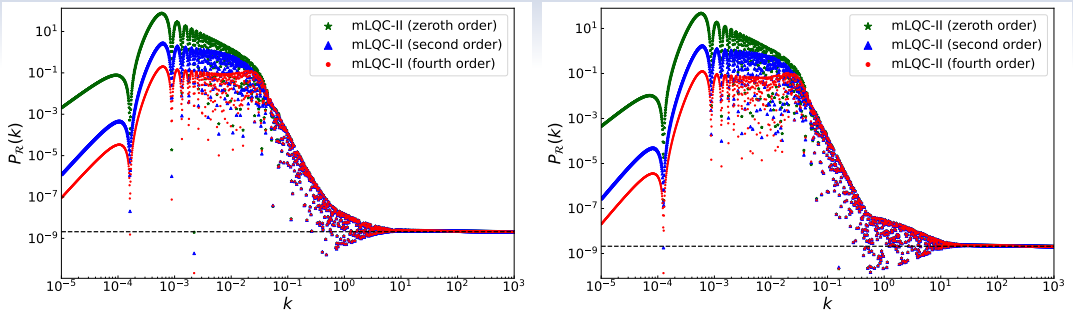

Figure: The primordial power spectrum for mLQC-II with different adiabatic initial states (zeroth, second, and fourth order) in the hybrid approach (left) and the dressed metric (right) approaches while $t = -10^6$, $\phi_B = -1.54$, and $m = 2.7 \times 10^{-6}$.

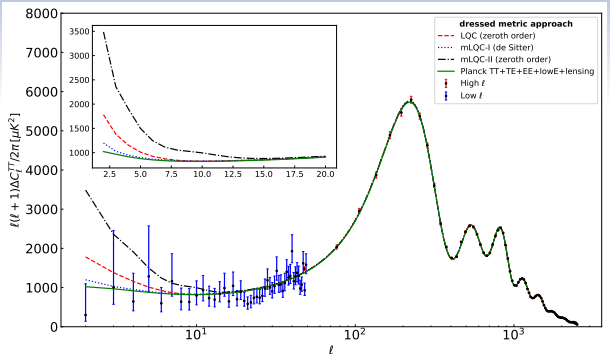

Figure: The angular power spectrum predicted by LQC models in the case of the dressed metric approach, while zeroth order adiabatic initial states are used for LQC and mLQC-II and de Sitter initial state is used for mLQC-I. The black dots are the Planck 2018 temperature angular power spectrum, with blue error bars for low l multipoles and red error bars for large l multipoles. The green curve is the ΛCDM angular power spectrum best fit to Planck 2018 data.

Summary

This lecture mainly addresses the following content regarding the modified LQC models.

- The effective dynamics: the modified FR equations, the inflationary scenario and the qualitative dynamics.
- The linear perturbation theory in mLQCs: the dressed metric approach, the hybrid approach and comparison of the primordial scalar power spectra from LQC and mLQCs.

Thank you for your attention and time!